Vibrational Energy Relaxation and Spectral Diffusion in Water and Deuterated Water

John C. Deàk,[†] Stuart T. Rhea, Lawrence K. Iwaki,[‡] and Dana D. Dlott*

School of Chemical Sciences, University of Illinois at Urbana-Champaign, Box 01-6 CLSL, 600 South Goodwin Avenue, Urbana, Illinois 61801

Received: December 24, 1999; In Final Form: March 14, 2000

In the broad water stretching band (2900−3700 cm^{-1}), frequency-dependent vibrational energy relaxation (VER), and spectral diffusion both occur on the time scale of a few picoseconds. Ultrafast IR−Raman spectroscopy of water is used to study both processes. VER is also studied in solutions of HDO in D_2O (HDO/D_2O). The OH stretch (ν_{OH}) lifetime for water and HDO is ∼1 ps. The OD stretch (ν_{OD}) lifetime for D_2O is ∼2 ps. Stretch decay generates substantial excitation of the bending modes. The lifetimes of bending vibrations (δ) in H_2O, HDO, and D_2O can be estimated to be in the 0.6 ps ≤ T_1 ≤ 1.2 ps range. ν_{OH} decay in water produces δ_{H_2O} with a quantum yield 1.0 ≤ ϕ ≤ 2.0. In HDO/D_2O solutions, ν_{OH}(HDO) decay generates ν_{OD}(D_2O), δ_{HDO}, and δ_{D_2O}. The quantum yield for generating ν_{OD}(D_2O) is $\phi \approx 0.1$. The quantum yield for generating both δ_{HDO} and δ_{D_2O} is $\phi \geq 0.6$. Thus, each ν_{OH}(HDO) decay generates at minimum 1.2 quanta of bending excitation. After narrow-band pumping, the distribution of excitations within the stretch band of water evolves in time. Pumping on the blue edge instantaneously (within ∼1 ps) generates excitations throughout the band. Pumping on the red edge does not instantaneously generate excitations at the blue edge. Excitations migrate uphill to the blue edge on the 0−2 ps time scale. The fast downhill spectral diffusion is attributed to excitation hopping among water molecules in different structural environments. The slower uphill spectral diffusion is attributed to evolution of the local liquid structure. Shortly after excitations are generated, an overall redshift is observed that is attributed to a dynamic vibrational Stokes shift. This dynamic shift slows down the rate of excitation hopping. Then energy redistribution throughout the band becomes slow enough that the longer VER lifetimes of stretch excitations on the blue edge can lead to a gradual blue shift of population over the next few picoseconds.

1. Introduction

In this paper we investigate vibrational energy relaxation (VER) and vibrational spectral diffusion resulting from excitation of stretching transitions of water and deuterated water, using ultrafast IR−Raman spectroscopy.[1−4] VER in water is especially complicated because within the broad water stretching transition, VER rates are frequency-dependent, and VER and spectral diffusion compete on the same time scale of a few picoseconds. The incoherent anti-Stokes Raman technique used here is especially useful because we simultaneously observe all water excitations throughout the stretching and bending regions. Several important processes seen here have never been observed previously. These include the dynamics of stretching vibrations in water and heavy water, and the dynamics of bending vibrations in water, heavy water and solutions of HDO in D_2O. We detect the appearance and subsequent decay of OH stretching excitations pumped by ultrashort mid-IR laser pulses, and we observe for the first time the appearance and subsequent decay of daughter bending vibrations generated by VER of the stretching excitations.

The principal significance of the VER measurements lies in the opportunity to improve water potential energy surfaces, which as we shall see do not adequately explain water VER. VER is sensitive to higher order anharmonic terms in the potential expansion,[5,6] providing a critical test of the accuracy of the potential surface. In addition, VER of water might play a role in aqueous chemical reaction dynamics.[7−9] The principal significance of the vibrational spectral diffusion measurements lies in the ability to probe the time evolution of the environment near a vibrational excitation,[10−13] which addresses the continuum versus multicomponent environment controversy, and which helps to understand aqueous chemistry and solvation,[14,15] and in the ability to probe the highly efficient intermolecular vibrational energy transfer and the exciton-like nature of the OH stretch excitation in water.[16,17]

Almost all recent studies of water vibrational dynamics relevant to the present work have involved ultrafast mid-IR two-color pump−probe experiments (hereafter "pump−probe") of OH stretch transitions (denoted ν_{OH}) in the approximate spectral range 2800−3800 cm^{-1}, of *dilute solutions* of HDO in D_2O (hereafter HDO/D_2O). There are almost no data on water itself, except for some vibrational saturation measurements[18] and a very recent report[13,16] of the time-dependent polarization anisotropy decay. It is worth emphasizing that HDO/D_2O is in many ways totally different from water. Water is the liquid of life; heavily deuterated water is a poison. Water (symmetry group C_{2v})[19] and HDO (symmetry group C_1)[19] have qualitatively different vibrational spectra.[19,20] In HDO/D_2O, OH and OD stretching vibrations are nearly localized on their respective bonds, whereas the symmetric stretch (ν_s) and antisymmetric stretch (ν_{as}) vibrations of water are delocalized over the molecule. In water, ν_{OH} excitations undergo rapid intermolecular

* To whom correspondence should be addressed. E-mail: dlott@scs.uiuc.edu.

† Present address, Procter and Gamble Corp., 11801 E. Miami River Road, Ross, OH 45061.

† Present address, National Institute of Standards and Technology, Gaithersburg, MD.

10.1021/jp994492h CCC: $19.00
Published on Web 05/03/2000

hopping to nearby water sites,[13,16] whereas in dilute solutions of HDO/D_2O, ν_{OH} excitations are localized on one molecule. HDO in D_2O has a mixture of hydrogen bonds and deuterium bonds which are a bit stronger, whereas water has only hydrogen bonding, and so on.

In 1991, the first reports of VER in HDO/D_2O appeared. Graener, Seifert, and Laubereau[21] used the pump−probe method with 11 ps pulses to obtain a ν_{OH} lifetime of 8 ps. Vodopyanov[18] made intensity-dependent transmission measurements of 110 ps mid-IR pulses through water and HDO/D_2O, to estimate the saturation intensity and the VER lifetime. The ν_{OH} lifetime was estimated at 0.3−0.6 ps for HDO/D_2O, and for water <3 ps. In 1996, Rey and Hynes[22] used molecular dynamics to investigate VER of HDO/D_2O. They computed the rates of all possible transitions and the computed ν_{OH} lifetime was found to be in agreement with ref 21. The principal VER pathway of ν_{OH} in HDO/D_2O was said to be

$$\nu_{OH} \rightarrow \delta(\upsilon=2) \rightarrow \delta\ (\upsilon=1) \rightarrow \text{ground}$$

where δ indicates a bending excitation.

Recently measurements have significantly improved due to advances in laser technology. It is now clear that the 8 ps lifetime was erroneous. The ν_{OH} lifetime varies somewhat across the ν_{OH} band,[23] so it is impossible to specify an exact lifetime, but $T_1 \sim 1$ ps (0.7 and 1.0 ps have been frequently reported[10−13,23−26]). In 1998, Woutersen and Bakker showed that VER of HDO/D_2O became slightly faster as the temperature was decreased.[24] Nienhuys et al.[26] in 1999 studied ν_{OH} excitations in HDO/D_2O with one-color and two-color pump probe. They found the initial decay of ν_{OH} was somewhat faster than the repopulation of the ground state. They inferred the existence of a daughter vibration created by ν_{OH} decay, with a lifetime in the 0.5−2.0 ps range. On the basis of temperature and frequency-dependent VER measurements, they claimed that hydrogen bond excitations were the dominant product of ν_{OH} VER, in contrast to the bending excitations predicted by Rey and Hynes.[22]

Orientational dynamics of HDO/D_2O have been studied via the mid-IR polarization anisotropy decay. Woutersen et al.[23] in 1997 saw two components in the anisotropy decay, 0.7 and 13 ps, whose relative amplitudes varied across the ν_{OH} band. These observations were attributed to different rates of molecular rotation in different hydrogen bonding environments. Woutersen's 1999 Ph.D. thesis[13] provides an excellent summary of the field prior to the present work. Recently new polarization anisotropy decay measurements were reported.[13,16] The polarization anisotropy decay rate increased with increasing HDO concentration in HDO/D_2O solutions, which was attributed to Förster transfer of ν_{OH} excitations among HDO molecules in different orientations.[16] A measurement of a <100 fs anisotropy decay in the ν_{OH} band of neat water was attributed to very fast intra- and intermolecular vibrational energy hopping. Intermolecular vibrational energy transfer is ordinarily thought to be inefficient in polyatomic liquids and solutions, where VER is usually faster than hopping between adjacent molecules, although intermolecular transfer can be quite efficient in the long-lived vibrations of diatomic liquids or solutions.[27,28] A few studies have shown moderately efficient intermolecular transfer in polyatomic solutions provided there are strong interactions such as hydrogen bonds between donors and acceptors.[29,30] Thus, it is a very interesting and possibly unique feature of water that intermolecular vibrational transfer is so efficient that it can effectively compete with a ~1 ps VER decay rate.[17]

Spectral diffusion studies of HDO/D_2O began in 1998, with Laenen et al..[10,31] Their pump−probe experiments saw narrow (~45 cm^{-1}) features in the ν_{OH} band, which were claimed to be spectral holes burnt into the vibrational transition. Spectral diffusion was observed, which was interpreted as arising from structural evolution among a small number of local structures, each corresponding to a characteristic Gaussian subband underneath the broader ν_{OH} transition. The interpretation of narrow spectral holes was criticized by Woutersen,[13] who argued that these "holes" had nothing to do with population dynamics, but instead were artifacts arising from coherent coupling between the pump-and-probe pulses. Woutersen[13] presented calculations which showed that a complete theoretical treatment of the coupling between pump-and-probe pulses could reproduce all of Laenen et al.'s results without sharp spectral holes.

In 1999, Gale et al.[12] used 150 fs pulses to study spectral diffusion in HDO/D_2O. Pumping ν_{OH} at either the red or blue edge generated an initially narrowed population distribution at each respective edge, which moved toward the band center in ~1 ps. The results were interpreted using the formalism of Bratos and Leicknam,[32] who asserted that the experiment probes the kinetics of interconversion among hydrogen bonds of different lengths. In 1999, Woutersen and Bakker reported the observation of a fast red shift in the spectrum of $\upsilon = 1$ excitations of ν_{OH} in HDO/D_2O, termed a "vibrational dynamic Stokes shift".[25] The $\nu_{OH}(0) \rightarrow 1$ band was pumped, and the $\nu_{OH}(1) \rightarrow 0$ transition was probed. Over the course of ~500 fs, the emission redshifted by about 70 cm^{-1}. The observed redshift of ~70 cm^{-1} in HDO/D_2O was said to occur because hydrogen bonding in the excited $\upsilon = 1$ state is somewhat stronger than in the ground $\upsilon = 0$ state. This Stokes shift appeared to contradict the work of Gale et al.,[12] who did not see a net red shift. However Woutersen and Bakker[25] pointed out that with the pump−probe technique used by Gale et al.[12] a detailed mathematical model is needed to extract the Stokes shift of the excited vibrations against the background of the unshifted population hole (depletion of the $0 \rightarrow 1$ transition) and the overtone ($1 \rightarrow 2$) transition.

The IR pump, incoherent anti-Stokes Raman probe technique used here has been discussed extensively[1,2,33] and compared to pump−probe spectroscopy.[2,34] In both techniques, a mid-IR pump pulse excites the selected vibrational transition. In pump−probe, the probe pulse is sensitive to $\upsilon = 0 \rightarrow 1$ transitions via induced saturation, $1 \rightarrow 2$ transitions via excited-state absorption, and $1 \rightarrow 0$ transitions via stimulated emission.[10,11] In IR−Raman, anti-Stokes probing is an induced emission process sensitive only to vibrational excited states. When fundamental excitations alone are present, only $\upsilon = 1 \rightarrow 0$ transitions are observed. When overtone excitations are present, they are seen as $2 \rightarrow 1$ transitions.[3,35] IR−Raman with parallel pump-and-probe polarizations is insensitive to orientational relaxation for strongly polarized Raman transitions.[4] The depolarization ratios for OH and OD stretching transitions of water and heavy water vary somewhat across the band, but are always considerably below the ratio of 6:7 for a depolarized transition,[36] so the rotational contribution to our IR−Raman signals in water is minimal. There are subtle differences in measuring spectral diffusion by pump−probe or by IR−Raman, similar to the way that absorption hole burning spectroscopy differs from fluorescence line narrowing.[37]

In the rest of this paper, we briefly discuss some relevant properties of the water vibrational spectrum and the experimental method. Then we present and discuss results concerning VER and vibrational spectral evolution in the ν_{OH} band of water, and VER resulting from ν_{OH} pumping of HDO/D_2O and ν_{OD} pumping of heavy water.

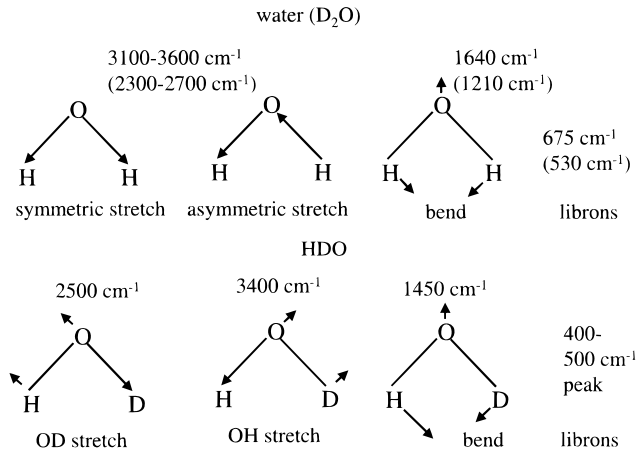

Figure 1. Normal modes of water and heavy water (D_2O wavenumbers in parentheses) and HDO. In water and heavy water, the symmetric stretch, asymmetric stretch and bending first overtone transitions all overlap. In HDO the OH stretch, OD stretch and bend first overtone are separated.

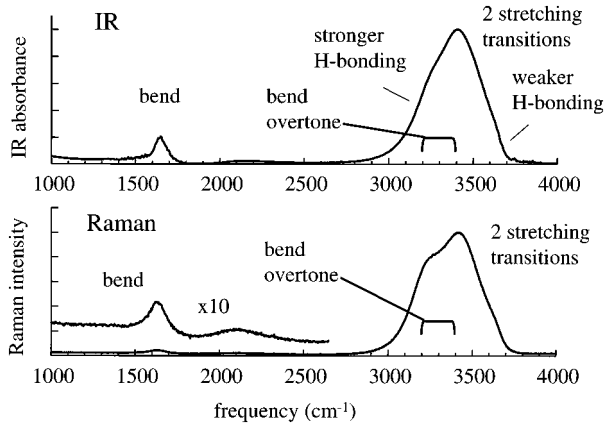

Figure 2. Mid-infrared (mid-IR) and Raman spectra of ambient liquid water. Hydrogen bonding becomes weaker at higher wavenumber. The broad transition in the 2900−3700 cm^{-1} range includes two stretching transitions and the bend first overtone. The approximate location of the bend overtone is indicated. The bend fundamental is at 1640 cm^{-1}.

2. Vibrational Spectroscopy of Water

Vibrational spectroscopy of water has been reviewed extensively.[20] Figure 1 shows the three normal modes of water and heavy water, ν_s, ν_{as}, and δ. Figure 2 shows the IR and Raman spectrum of water. A broad transition in the 3100−3600 cm^{-1} range involves a mixture of ν_s, ν_{as}, and bend first overtone character, which varies with wavenumber in a manner not yet fully understood.[38] The approximate location of bend overtone transitions deduced from gas-phase data[19] is denoted in Figure 2. The ν_s and ν_{as} fundamentals of bare water molecules in the vapor, where there is no hydrogen bonding, lie at the extreme blue edge of the stretching band (3652 and 3756 cm^{-1}. respectively).[19] It is well-known that the redshift within the stretching band correlates well to increasing strength of hydrogen bonding.[20] Excitations near the red edge of the band (e.g., ∼3000 cm^{-1}) have the strongest hydrogen bonding. Excitations near the blue edge of the band (e.g., ∼3600 cm^{-1}) have the weakest hydrogen bonding.

The bend fundamental in water is near 1640 cm^{-1}.[19] The ratio of stretch to bend Raman cross sections, $\sigma_R(\nu)/\sigma_R(\delta) \approx 40$, as seen in Figure 2 and in ref 39. A feature near 675 cm^{-1} [36] is assigned to librational modes. In the Raman, this libron peak is about as intense as the bend.[39] Heavy water (not shown) is similar but overall lower in frequency. The broad stretching region in heavy water (2300−2700 cm^{-1}) includes both ν_s and ν_{as} and the bend first overtone. The bend fundamental frequency ∼1210 cm^{-1}.[36]

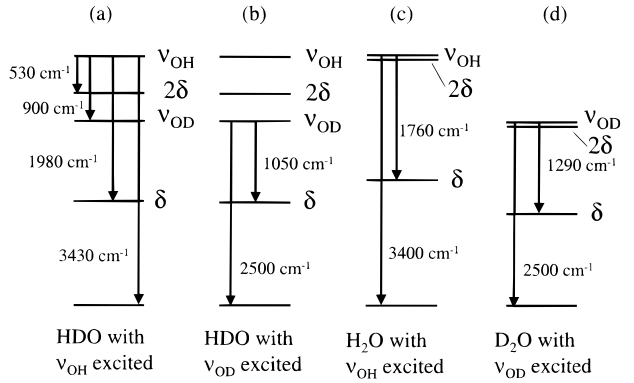

Figure 3. Energy level diagrams for water vibrational energy relaxation (VER). Each broad water transition is denoted by a line at the center frequency. 2δ denotes the bend first overtone. In water and heavy water, ν indicates both symmetric and asymmetric stretching vibrations.

As shown in Figures 1 and 3, HDO is fundamentally different. Instead of ν_s and ν_{as} excitations delocalized over the molecule, there are ν_{OH} and ν_{OD} excitations principally localized on either bond that are somewhat narrower than the water and heavy water stretching transitions.[40] The ν_{OH} and ν_{OD} and bend first overtone transitions (bend fundamental frequency ∼1450 cm^{-1})[19] do not all overlap, as in water and heavy water, but instead are well separated in HDO. Energy level diagrams for H_2O, D_2O, and HDO are shown in Figure 3, where the broad transitions are represented as thin lines at the central vibrational frequency.

3. Experimental Section

A. Laser System. In our experiments on liquid water at ambient temperature, the fwhm of the time response is 1.2 ps and the fwhm of the spectral response is 55 cm^{-1}.[33,41] The IR and Raman pulses are generated by a 2-color optical parametric amplifier pumped by a 1.5 ps Ti:sapphire laser system.[33,41] The pump pulses (2800−3650 cm^{-1}, ∼0.8 ps, 35 cm^{-1} fwhm, ∼40 μJ, ∼200 μm diameter) and probe pulses (532 nm, ∼0.8 ps, 45 cm^{-1} fwhm, ∼10 μJ, ∼150 μm diameter) were focused on a jet of flowing water ∼50 μm thick. The anti-Stokes signal was acquired by a spectrograph and a high quantum efficiency charge-coupled array detector (CCD). A spectrum is obtained by averaging for ∼15 min. Several spectra are obtained over several days, which are averaged together. Each displayed spectrum is the result of an integration time ranging from 0.5 to 5 h, where the longer integration times were used for experiments such as water bend detection, where the signal levels were lower.

B. Geometrical Effects. The sample geometry and the optical geometry[33] are depicted in Figure 4. The water jet is ∼50 μm thick. The jet is optically thick with respect to the pump pulse, but optically thin with respect to the nonresonant Raman probe. As the pump pulse is tuned in frequency, the absorption length varies, but the number of vibrational excitations seen by the probe remains roughly constant, and about equal to the number of mid-IR photons in the pump pulse (∼7×10^{14}).

In this counterpropagating geometry, a small degradation in temporal response occurs as a result of the finite sample thickness.[33] To illustrate, assume a 1.2 ps instrument response due to a mid-IR and a visible pulse each 0.85 ps in duration.

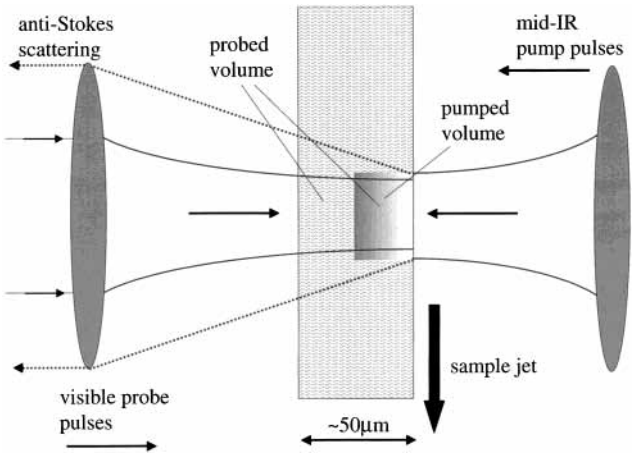

Figure 4. Sample and collinear optical geometry used in IR−Raman experiments, adapted from ref 33.

Then the temporal degradation in the worst case (say a sample transit time of 250 fs through an ~50 μm thick sample, with refractive index 1.5), is only ~3%. The instrument response would be lengthened to ~1.23 ps. Thus, temporal degradation due to geometry is negligible.

The water jet can be replaced by a 50 μm thick crystal of KTP (potassium titanyl phosphate). Since KTP is noncentrosymmetric, coherent sum-frequency generation (SFG) is dipole-allowed. Some of the SFG signal is scattered into the detector. Monitoring the SFG signal as a function of relative delay provides information about the apparatus time and spectral response, a type of FROG (frequency-resolved optical gating) measurement.[42]

C. Coherent Coupling Artifacts. Coherent coupling artifacts, which appear only when the pump and probe pulses overlap in time, are well-known in ultrafast spectroscopy,[43] but have not been discussed much in the case of IR−Raman experiments[44] until recently.[45] The most important artifact in our experiments occurs at the sum frequency, near the location where we observe the vibration being pumped. When ω_v is the (mid-IR) frequency of the vibration being pumped and ω_L is the frequency of the Raman probe pulse, the pumped vibration is detected near the sum-frequency $\omega_L + \omega_v$. Sum-frequency generation (SFG) due to coherent interactions between the pump and probe pulse may be either incoherent (nonphase matched and nondirectional) or coherent (phase-matched and directional). The incoherent part in an isotropic medium is sometimes called elastic second-order nonlinear light scattering.[46,47] In our experimental geometry, we avoid the possibility of directly detecting coherent SFG signals, but it is possible that a small part of a coherent signal is scattered into our detector by the sample. In the dipole approximation, coherent SFG is forbidden in bulk water, but coherent SFG at the water−air interface is allowed.[48] However in the present experimental geometry with both pulses polarized in the interface plane, that surface signal will vanish. Higher order terms in the multipole expansion, principally the quadrupole term, do permit both bulk and surface SFG. We cannot at present experimentally distinguish between incoherent SFG and scattered coherent SFG. Both processes will produce an SFG artifact that can distort the spectrum and obscure the dynamics of the build-up and decay of the parent vibration[33,45] near the pump wavenumber.

Inelastic second-order nonlinear light scattering [46,47] might produce artifacts near zero time delay at frequencies other than the sum frequency, that could distort the spectrum at locations other than the location of the pumped vibration. Of specific

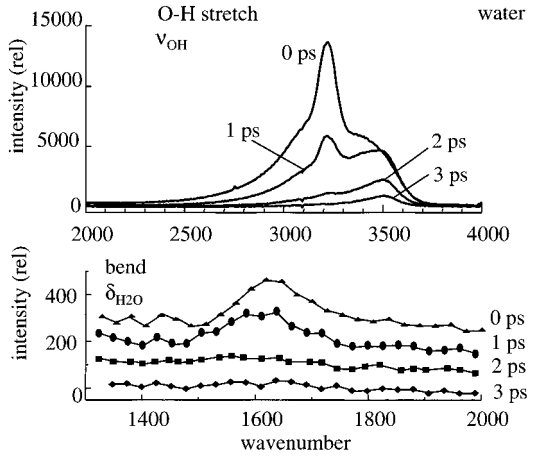

Figure 5. Anti-Stokes Raman transients for water pumped in the ν_{OH} band at 3250 cm^{-1}. The sharp feature near $t = 0$ is an artifact caused by sum frequency generation (SFG). Excitations on the blue edge of the ν_{OH} band decay slowest. The ν_{OH} lifetime is ~1 ps. The spectra in the bending region are offset for clarity. Excitation of the bending vibration is evident near $t = 0$. The bend lifetime is in the 0.6−1.2 ps range. The quantum yield for bend generation via stretch decay is $1.0 \leq \phi \leq 2.0$.

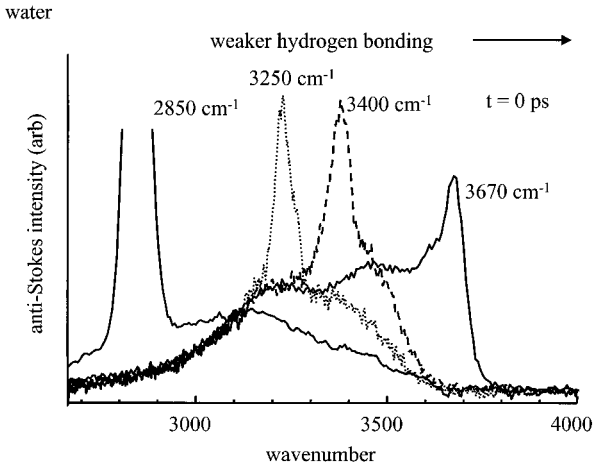

Figure 6. Anti-Stokes transients for water pumped at four different mid-IR frequencies in the ν_{OH} band, normalized to match the intensities at 3100 cm^{-1}. These transients reflect the distribution of ν_{OH} excitations pumped by narrow band (~35 cm^{-1}) mid-IR pulses plus any spectral diffusion occurring during the ~1.2 ps pulse. Higher energy pumping generates excitations throughout the band. Lower energy pumping produces a narrowed distribution with fewer excitations at higher energy. The sharp feature is an artifact caused by sum frequency generation (SFG).

concern for observing ν_{OH} excitations would be processes that generated light at $\omega_L + \omega_v \pm \omega_{libr}$, where ω_{libr} is a water libron (typically ω_{libr} is in the 300−800 cm^{-1} range). The effects of inelastic second-order scattering turn out not to be a problem in the present experiments. Terhune, Maker, and Savage[46] have shown that the inelastic second-order scattering due to water librons is at most ~3% of the elastic scattering. Our experiments show that the SFG artifact is comparable in intensity to the desired incoherent anti-Stokes signal, so the inelastic second-order scattering ought to be inconsequential. That is demonstrated in the present work by referring to Figure 6, where water is pumped at 3670 cm^{-1}, where the SFG ($\omega_L + \omega_v$) has been moved to the blue edge of the transition. Looking past the blue edge, we see no significant inelastic scattering ($\omega_L + \omega_v + \omega_{libr}$). The same is true with red edge pumping looking to the red of the red edge for inelastic scattering at ($\omega_L + \omega_v - \omega_{libr}$).

4. Results

A. Water. *Vibrational Energy Relaxation.* Transient water spectra with ν_{OH} pumping at 3250 cm^{-1} are shown in Figure 5. The sharp feature at 3250 cm^{-1} is an SFG artifact. The excited vibrations in the ν_{OH} region vanish in a few picoseconds. The intensity decline, ignoring the artifact, gives a lifetime of ~1 ps for ν_{OH} of water, the same as that reported for ν_{OH} in HDO/D_2O.[10−13,23−26] As time increases, the center of the vibrational population distribution shifts toward the blue, so at longer times (e.g., 3 ps), most of the excitations that remain are near the blue edge of the transition, where hydrogen bonding is the weakest.

Figure 5 also shows the water bend transient. In this figure, which took many hours of signal averaging, the thermal background anti-Stokes signal has been removed by baseline subtraction. Transient bend excitation is seen only near $t = 0$. The bend decay appears to be limited by the apparatus time response, so it is problematic to determine the bend lifetime by direct time resolution of the signal. Similarly, it is problematic to determine the bend-to-stretch quantum yield ϕ by the usual method of comparing anti-Stokes intensities and Raman cross sections,[3,49,50] because bend excitations are decaying during the pulse. Any determination of the quantum yield which relies on the instantaneous bend and stretch intensities will be an *underestimate* of the total bend population generated by stretch VER. For water, Figure 2 shows the ratio of stretch-to-bend Raman cross sections is about 40, and is about the same as for D_2O.[39] At $t = 0$ in Figure 5, the amplitude of the stretch transition (in relative units, disregarding the SFG artifact) is ~7000, and the amplitude of the bend transition is ~180, so the ratio of stretch to bend amplitudes is 39. Therefore, at minimum 1.0 bend quantum is generated by each stretch decay. Energy conservation precludes the possibility of creating more than two bends per stretch, so an upper limit for ϕ is 2.0. Thus, the quantum yield for bend generation by stretch VER is $1.0 \leq \phi \leq 2.0$. If the bend lifetime were <0.6 ps, then more than one-half of the bending excitations would have decayed during the laser pulse. The quantum yield would be more than twice what is determined using the instantaneous intensity ratio, and the quantum yield would exceed 2.0. Thus, we can provide a lower limit of 0.6 ps for the bend lifetime, and therefore an estimate of $0.6 \leq T_1 \leq 1.2$ ps.

Spectral Diffusion. Figure 6 shows the effects of tuning the pump pulses. These ν_{OH} water spectra are scaled to match the intensities at 3100 cm^{-1}. The $t = 0$ spectra are due to excitations produced by the spectrally narrow (~35 cm^{-1} fwhm) pump pulses plus any spectral diffusion occurring during the ~1 ps pump pulse. As the pump pulse is tuned, the SFG artifact in Figure 6 follows, and it always has the same spectral width (~55 cm^{-1}) as the apparatus spectral response.

When water is pumped in the higher frequency part of the band (e.g., 3670 cm^{-1}), excitations are instantaneously (i.e., within ~1 ps) generated throughout the band. But when water is pumped at lower frequencies, excitations are not instantaneously generated at the blue edge. For example, with 2850 cm^{-1} pumping, excitations are generated in the red edge and in the middle of the band (i.e., in the 2900−3200 cm^{-1} range), but the population distribution tails off toward the blue so that few excitations are generated above 3300 cm^{-1}. When water is pumped at 3250 or 3400 cm^{-1}, excitations are generated at the red edge and in the middle of the band, but few excitations are generated above 3500 cm^{-1} (Figure 6). These results demonstrate that the ν_{OH} transition of water is inhomogeneously broadened, and that downhill (toward the red) spectral diffusion is faster than uphill (toward the blue) spectral diffusion.

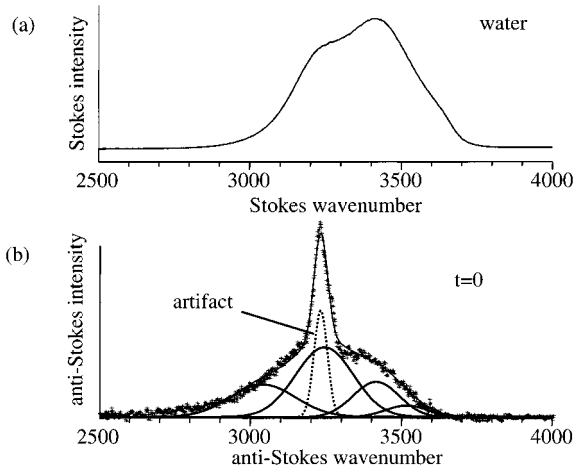

Figure 7. (a) Stokes Raman spectrum of water. (b) An anti-Stokes transient at $t = 0$ with 3250 cm^{-1} pumping. The anti-Stokes transient ($v = 1 \rightarrow 0$) is redshifted by ~120 cm^{-1} from the Stokes spectrum ($v = 0 \rightarrow 1$) due to a dynamic vibrational Stokes shift. The transient's shape is characterized by fitting it to four Gaussian subbands plus one Gaussian for the SFG artifact.

Some uphill spectral diffusion is demonstrably slower than our time resolution. It is well-known that the water stretching spectrum can be fit to a function consisting of four Gaussian subbands,[20] as shown in Figure 7a, where the fit is indistinguishable from the data. We fit all our transient data to four subbands solely to quantify the spectral evolution; our available data do not resolve the issue of whether these subbands represent well-defined local structures with characteristic spectra, as suggested previously.[10,11]

Figure 7b shows a fit to a typical transient anti-Stokes spectrum ($t = 0$ with 3250 cm^{-1} pumping). All transient spectra were accurately fit with the same four subbands plus an additional Gaussian near $t = 0$ to represent the SFG artifact. The major subbands were centered at 3250 and 3400 cm^{-1}; the minor subbands at 3500 and 3040 cm^{-1}. Figure 8 shows results of the Gaussian subband analysis for water pumped at 3250 and 3400 cm^{-1}. With 3400 cm^{-1} pumping (Figure 8a), the spectrum hardly evolves with time. ν_{OH} excitations instantaneously populate the two major subbands, which decay in concert to approximately maintain the band's shape as time increases (Figure 8a). There is a small build up at early time of the minor 3500 cm^{-1} band. This band decays a bit more slowly than the others, resulting in the gradual shift toward the blue seen in Figure 5, caused not by spectral diffusion but by the slower VER of 3500 cm^{-1} excitations.

When water is pumped at 3250 cm^{-1} (Figure 8b), the major 3400 and minor 3500 cm^{-1} subbands are not filled instantaneously. Figure 8b shows a net uphill movement of population on the 0−2.0 ps time scale, principally due to transfer from the major 3250 cm^{-1} subband to the major 3400 cm^{-1} subband. The gradual blue shift discussed above, due to frequency-dependent VER, is seen here as well.

Dynamic Stokes Shift. Our transient anti-Stokes spectra (e.g., Figure 7b) are noticeably redshifted from static Stokes spectra (Figure 7a), when both are plotted against wavenumber. This redshift is attributed to the dynamic vibrational Stokes shift, as discussed in ref 25. The vibrational Stokes shift is the frequency red shift between the $0 \rightarrow 1$ transition probed by Stokes Raman and the $1 \rightarrow 0$ transition probed by transient anti-Stokes Raman. The red shift in water is 120 (±30) cm^{-1}, determined by

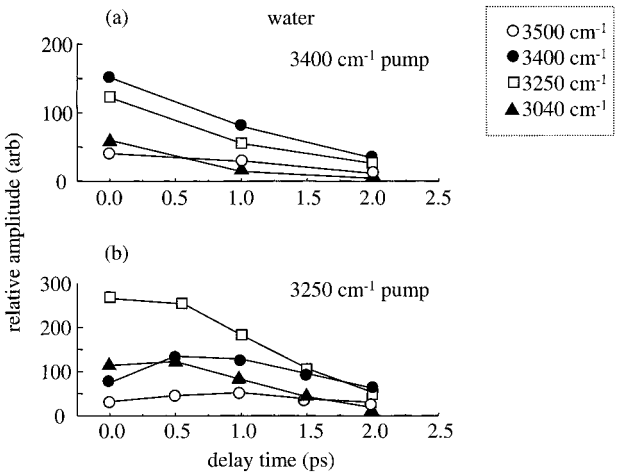

Figure 8. Time-dependent amplitudes of Gaussian subbands for water anti-Stokes transients with two pump frequencies. (a) With 3400 cm^{-1} pumping, the two major subbands at 3250 and 3400 cm^{-1} are populated together and decay nearly in concert, so the shape of the bulk of the band changes little with time. Some energy transfer to the minor 3500 cm^{-1} subband is observed. The minor 3500 cm^{-1} component decays more slowly than the others, so the band shape at longer times is blueshifted due to frequency-dependent VER. (b) With 3250 cm^{-1} pumping, there is significant spectral diffusion as shown by a substantial transfer of energy from 3250 to 3400 cm^{-1}.

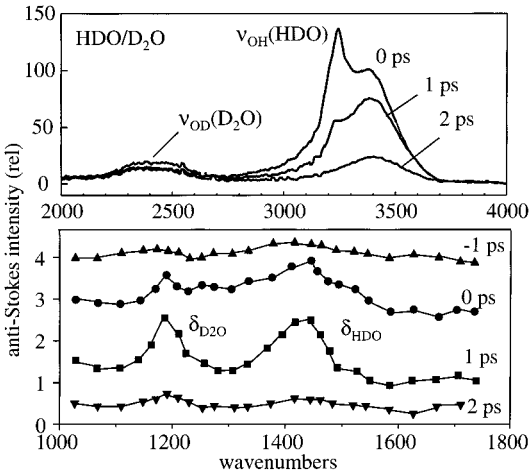

Figure 9. Anti-Stokes Raman transients for HDO in D_2O (8% HDO) with ν_{OH} pumping. About 10% of the ν_{OH} decays generate $\nu_{OD}(D_2O)$ excitations. The spectra in the bending region are offset for clarity. About equal amounts of bending excitations of HDO and D_2O are observed. The quantum yield for generation of bending excitations via stretch decay is $1.2 \leq \phi \leq 2.0$.

superimposing the spectra in Figures 7a and 7b and redshifting 7a for the best overall fit. The error bar is an estimate based on the range of redshifts that adequately fits the data. The value for water is definitely greater than the 70 cm^{-1} reported for HDO/D_2O.[25] We do not see the ~0.5 ps dynamic Stokes shift *in real time*, as in ref 25, where 0.2 ps pulses were used. However the redshift is easier to see with anti-Stokes Raman scattering than with pump−probe. Raman sees only the redshifted $1 \rightarrow 0$ transition, whereas pump−probe signals require mathematical analysis[25] to separate the redshifted $1 \rightarrow 0$ transition from the unshifted population hole (depletion of the $0 \rightarrow 1$ transition) and the overtone ($1 \rightarrow 2$) transition.[12]

B. HDO and Heavy Water. Figure 9 shows data on HDO/D_2O. Owing to the low sensitivity of Raman measurements, we must use higher concentrations of HDO than is typical in pump−probe experiments.[13,16] Our sample is 8 mol % H_2O in D_2O (4.4 M HDO). This concentration was chosen to give samples that are 90% pure. There is 8% HDO, 0.7% H_2O and 91.3% D_2O in the sample. Thus, the ν_{OH} transition is 91% pure HDO (9% H_2O), and the ν_{OD} transition is 91% D_2O (9% HDO). Woutersen's data[13,16] shows there is a bit of intermolecular vibrational energy transfer at this concentration, which is totally absent at the typical 0.5% concentrations (~0.3 M HDO) used in the cited[10−12,23−26] pump−probe experiments.

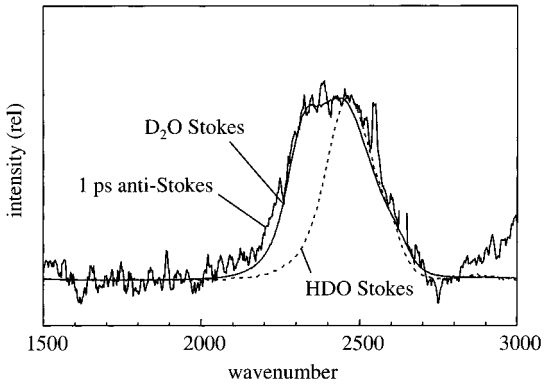

Figure 10. Comparison of a ν_{OD} anti-Stokes transient ($t = 1$ ps) in HDO/D_2O from Figure 9, with equilibrium Stokes spectra of HDO and D_2O (offset by ~100 cm^{-1} to account for the dynamic Stokes shift). HDO and D_2O are readily distinguishable. The transient is an excellent fit to the D_2O spectrum, showing that ν_{OH}(HDO) generates $\nu_{OD}(D_2O)$ but little ν_{OD}(HDO).

As shown in Figure 9, the ν_{OH} stretching transition of HDO decays in ~1 ps, as expected.[26] The time-dependent blue shift due to frequency-dependent VER is not as noticeable as in water (Figure 5), which is consistent with the report by Nienhuys et al.[26] that the VER lifetime in HDO/D_2O increases only a bit at the highest energies.

Several striking new features are seen in this isotopic mixture not seen in pure water (Figure 5). Even though the laser pumps ν_{OH}, we see some excitation of ν_{OD}, a significant and unexpected result. At the ν_{OD} signal peak, the ν_{OD} signal is about 10% of the ν_{OH} signal. Since these transitions have about the same cross section, the quantum yield for ν_{OD} generation by ν_{OH} is $\phi \approx 0.1$. We also see excitation of the two bending modes δ_{HDO} (~1450 cm^{-1}) and δ_{D2O} (~1210 cm^{-1}), but only in the 0−1 ps time range. In relative intensity units, the instantaneous maximum anti-Stokes intensities of ν_{OH}, δ_{HDO} and δ_{D2O} are 100, 1.5, and 1.5, respectively. Using the ratio of stretch-to-bend Raman cross sections $\sigma_R(\nu)/\sigma_R(\delta) \approx 40$, the quantum yield for δ_{HDO} generation from ν_{OH} is $\phi \geq 0.6$. The quantum yield for δ_{D2O} generation from ν_{OH} is also $\phi \geq 0.6$, so the total quantum yield for generating *any bending excitation* from a ν_{OH} decay is $1.2 \leq \phi \leq 2.0$, where the upper limit of $\phi \leq 2.0$ again is established by energy conservation.

In Figure 10, we compare an anti-Stokes ν_{OD} transient from Figure 9 to the equilibrium Stokes Raman spectra of D_2O and HDO in the ν_{OD} region. The HDO spectrum was obtained by adding a small amount of D_2O to H_2O, so that HDO would dominate D_2O. The equilibrium Stokes spectra are offset ~100 cm^{-1} to account for the vibrational dynamic Stokes shift. Figure 10 shows that, in the ν_{OD} region, HDO and D_2O are clearly distinguishable. The HDO spectra are characteristically narrower.[36] Comparison to the transient spectrum shows that the ν_{OD} excitations seen in the transients are overwhelmingly due to D_2O. If there is any excited HDO in Figure 9, it is buried under the D_2O signal. Since in Figure 9 we see both $\nu_{OD}(D_2O)$ and $\delta(D_2O)$ excitations after ν_{OH} pumping, there must be *intermolecular energy transfer* from HDO solute to D_2O solvent.

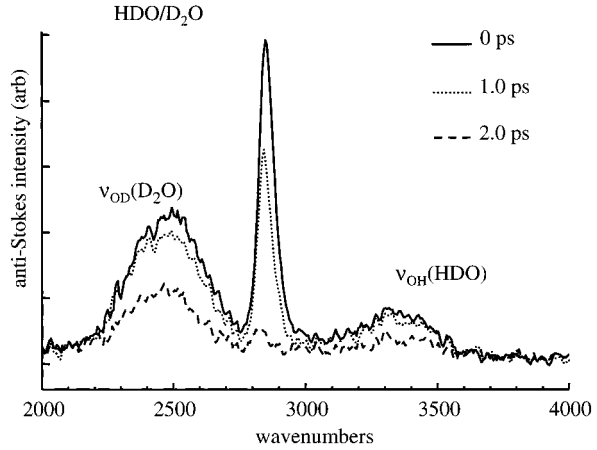

Figure 11. Anti-Stokes Raman transients for HDO in D_2O (8% HDO) pumped at a wavelength on the red edge of the ν_{OH} transition and the blue edge of the ν_{OD} transition. The sharp feature between the two transitions is an SFG artifact. The ν_{OH} excitations are almost entirely HDO and the ν_{OD} excitations are almost entirely D_2O. The ν_{OH} lifetime is ~1 ps and the ν_{OD} lifetime is ~2 ps.

In another experiment, our HDO/D_2O sample (4.4 M HDO) was pumped at 2850 cm^{-1}, which excites ν_{OH} of HDO on its red edge and ν_{OD} of D_2O on its blue edge. (In the ν_{OH} region there is no D_2O and in the ν_{OD} region there is only 10% HDO). The result is shown in Figure 11. The SFG artifact is now in the region between the two stretching transitions, demonstrating that it cannot possibly represent a population transient. At 2 ps when the ν_{OH} excitations are almost gone, some excited D_2O ν_{OD} excitations still remain. Using Figure 11, we can estimate the lifetime of D_2O stretching excitations, $T_1 \approx 2$ ps, to be about twice as long as ν_{OH} excitations of HDO or H_2O. This is the first determination of the stretch lifetime of D_2O.

5. Discussion

A. Coherent Artifact. Is the sharp feature near the pump number a coherent artifact or a narrow spectral hole burned into the ν_{OH} transition? The presence of a coherent artifact does not preclude the possibility of a narrow vibrational hole, since the latter may be buried under the former. Laenen et al.[10,11] claim their HDO/D_2O pump−probe experiments show narrow spectral holes. They seem to have never considered the possibility of coherent coupling artifacts, which strikes us as a serious omission. Woutersen[13] showed that essentially all the results of refs 10 and 11 could be reproduced without the need to postulate the existence of narrow spectral holes, by a model which correctly accounts for coherent coupling. That calculation is straightforward given the known mid-IR absorption cross sections, but a similar calculation is quite difficult for IR−Raman experiments since we do not accurately know the hyperpolarizabilities and quadrupolar contributions to the polarizabilities at the pump and probe frequencies and since it is difficult to assess the contribution of coherent SFG light scattered into the detector.

We attribute the sharp feature in Figures 5−7 and 9−10 to an SFG artifact[33,45] for the following reasons. (1) When the mid-IR pump is tuned to the edge of the water absorption (e.g., 2850 cm^{-1} in Figures 6 and 11), the sharp feature becomes much larger than the anti-Stokes signal from excited vibrations, which is opposite from what is expected for a vibrational hole. For hole burning, the depth of the hole ought to be increase with increasing IR cross section[37] near the center of the band. The SFG signal in Figures 6 and 11 could result instead from incoherent SFG generation in water by second-order elastic light scattering[46] or from coherent SFG generation due to coupling between the fields and the water quadrupoles that is scattered into our detector. When tuned just off resonance, the decrease in mid-IR cross-section would be offset by an increase in the interaction length. (2) If we purposely increase the surface area of our sample by making the water jet spray some tiny droplets, the sharp feature increases immensely in intensity, showing that surface SFG signals can be efficiently generated and detected in water. (3) Elastic second-order light scattering and coherent SFG processes are well-known to exist and have been widely studied, whereas the existence of sharp vibrational holes in water is based solely on an analysis[10,11] which did not consider the possibility[13] of artifacts. Occam's razor requires us to disprove the existence of SFG artifacts before we can believe we are seeing narrow vibrational holes.

B. Time-Dependent Line Shape of Water Stretching Vibrations. These are the first spectral diffusion experiments in water, which appear somewhat different from earlier measurements in HDO/D_2O. A notable difference between dilute solutions of HDO/D_2O and neat water is that ν_{OH} excitations are localized on HDO in the former, whereas ν_{OH} excitations in water should be viewed as either delocalized excitations of a disordered medium[51] or as excitations that hop rapidly among nearby sites in <100 fs.[13,16] In a recent study of spectral diffusion in dilute solutions of HDO/D_2O,[12] which had better time resolution than available here (0.15 ps vs 1 ps), pumping ν_{OH} at either the red edge or the blue edge instantaneously generated a narrowed population distribution at each respective edge. These ν_{OH} populations then diffused toward the band center in ~1 ps.[12]

The uphill spectral diffusion seen here after red edge pumping is quite similar to that seen in HDO/D_2O in ref 12 if we realize that due to our longer pulse duration, at the earliest times in our experiments we already see the results of ~1 ps of the spectral diffusion process. However, the downhill spectral diffusion in water after blue edge pumping is clearly faster than what is seen in HDO/D_2O. For this reason, we attribute the fast downhill spectral diffusion to intermolecular excitation transfer from regions of higher energy (weaker hydrogen bonding) to regions of lower energy (stronger hydrogen bonding). The slower uphill spectral diffusion might occur either as a result of thermally activated hopping from regions with stronger hydrogen bonding to regions with weaker hydrogen bonding, or by structural evolution of these regions due to liquid-state dynamics. We attribute the uphill process to structural evolution, because we see essentially the same uphill spectral diffusion as in HDO/D_2O where hopping is not possible.

The intermolecular hopping rate ought to be affected by the dynamic Stokes shift. The initial state produced by the laser is the bare vibron. Over the next ~0.5 ps, dressing[52] of the bare vibron occurs as the local structure becomes distorted in response to the stronger hydrogen bonding in the $v = 1$ state. The ~100 cm^{-1} shift associated with dressing is smaller than the width of the ν_{OH} band, so the dressing process probably does not entirely localize the vibron. Instead it just slows down the intermolecular transfer[52] after the first ~0.5 ps.

At longer times (2−3 ps), all the ν_{OH} excitations that remain are near the blue edge of the band. Presumably the VER lifetime on the blue edge is the longest. How can this be reconciled with the very fast downhill spectral diffusion observed in Figure 6? The most likely explanation is that downhill spectral diffusion due to vibrational energy migration slows down after the first

~0.5 ps in response to the structural distortion resulting from the dynamic Stokes shift. In the presence of this slower spectral diffusion, it becomes possible for frequency-dependent VER to produce a nonuniform blue-shifted population distribution within the band.

C. Pathways of Vibrational Energy Relaxation in Water. We should consider the possibility that bend excitation we see are produced by *direct laser pumping* of the bend first overtone[33,49] occurring while exciting stretch fundamentals. If it turns out the bends are daughter excitations generated by VER of the parent stretch excitations, then there are quite a few plausible VER mechanisms that could account for the >1.0 quanta of bend produced per stretch decay. These break down into two categories: (1) processes which generate exactly 2.0 bend quanta, either as bend first overtones or pairs of bend fundamentals on adjacent molecules, or (2) processes where some pathways generate two bend quanta while others generate just a single-bend quantum.

Gas-phase data shows the water $\delta(\upsilon=0\rightarrow2)$ first overtone transition at 3151 cm^{-1} and the $\delta(\upsilon=0\rightarrow1)$ fundamental transition at 1595 cm^{-1}.[19] The anharmonic redshift for the first overtone is thus ~40 cm^{-1}. First overtone excitations in IR−Raman experiments are observed via the $\upsilon = 2 \rightarrow 1$ transition.[35] The bend overtone transition should be redshifted by ~40 cm^{-1} relative to the bend fundamental transition, and it should have a Raman cross section twice as large.[35] In the present case, a combination of poor spectral resolution (here ~55 cm^{-1}) and broad line widths (here ~100 cm^{-1}) makes it impossible to spectroscopically distinguish the bending overtone from the bend fundamental. In this case bend overtones appear simply as fundamental excitations with twice the amplitude[3].

Following Rey and Hynes,[22] the "bath" is defined as consisting of water librations, excitation of hydrogen bonds, and lower frequency collective motions. The excess energy not explicitly listed here is dissipated into the bath. Energy level diagrams are shown in Figure 3c. Processes where the *laser itself* creates the bend excitation are

$$\nu_{OH} \Leftrightarrow \delta(\upsilon = 2) \rightarrow \delta(\upsilon = 1) \rightarrow \text{ground} \quad (1a)$$

$$\nu_{OH} \Leftrightarrow \delta(\upsilon = 2) \rightarrow \text{ground} \quad (1b)$$

In eq 1, the double-headed arrow is used to signify that the initial state is an admixture of stretch fundamental and bend overtone character. Although direct laser pumping of coupled stretch and bend overtone states has been recently observed in acetonitrile[53] and nitromethane,[33,49] we regard this as unlikely to account for the observed bending excitations because we see the wrong dependence on pump wavelength. We still observe bend excitation when we pump ν_{OH} at 3650 and 2850 cm^{-1}, far away from the 3200−3400 cm^{-1} range of bend overtone energies indicated in Figure 2

VER processes which generate bend overtones are

$$\nu_{OH} \rightarrow \delta(\upsilon=2) \rightarrow \delta(\upsilon=1) \rightarrow \text{ground} \quad (2a)$$

$$\nu_{OH} \rightarrow \delta(\upsilon=2) \rightarrow \text{ground} \quad (2b)$$

Processes which generate bend fundamental excitations only are

$$\nu_{OH} \rightarrow \delta(\upsilon=1) \rightarrow \text{ground} \quad (3)$$

and

$$\nu_{OH} \rightarrow 2\delta(\upsilon=1) \rightarrow \delta(\upsilon=1) \rightarrow \text{ground} \quad (4)$$

Process 3 alone makes only 1.0 quanta of bend excitation per stretch decay. Process 4 involves intermolecular vibrational energy transfer of energy. Although intermolecular transfer is usually regarded as inefficient, hydrogen bonding facilitates intermolecular transfer. For example, intermolecular transfer is particularly efficient in hydrogen bonded complexes of nitromethane and methanol.[30] Thus, one of either process 2 or 4 must occur in ν_{OH} relaxation. If these processes are dominant, exactly 2.0 bend quanta would be produced per ν_{OH} decay. Alternatively there might be a competition with process 3 which produces 1.0 bend quanta, and the quantum yield for bend production would be less than 2.0 but more than 1.0.

D. Pathways of Vibrational Energy Relaxation in HDO/D_2O. An energy level diagram for ν_{OH} decay in HDO is shown in Figure 3a. Rey and Hynes[22] claimed that process 2a dominates, with the bend lifetime being somewhat shorter than the stretch lifetime. The relative rates computed for process 2a, process 2b $\nu_{OH} \rightarrow \nu_{OD}$, and $\nu_{OH} \rightarrow$ ground, were 1, 0.006, 0.022, and 0.004, respectively.[22]

The new features of our data, which have not been predicted, are the generation of $\nu_{OD}(D_2O)$ with a quantum yield $\phi \approx 0.1$, and the generation of $\delta(D_2O)$ with a quantum yield $\phi \geq 0.6$. These products must be the result of intermolecular υ-to-υ energy transfer. Intermolecular transfer was not regarded as significant by Rey and Hynes.[22] However intermolecular processes are helped by each HDO molecule having several D_2O neighbors.[54] In addition, hydrogen bonding appears to facilitate intermolecular transfer.[30] The intermolecular excitation of $\nu_{OD}(D_2O)$ may occur via several routes,

$$\nu_{OH}(HDO) \rightarrow \nu_{OD}(D_2O) \rightarrow \quad (5a)$$

$$\nu_{OH}(HDO) \rightarrow \nu_{OD}(HDO) \rightarrow \nu_{OD}(D_2O) \rightarrow \quad (5b)$$

$$\nu_{OH}(HDO) \rightarrow \delta_{HDO}\,(\upsilon=2) \rightarrow \nu_{OD}(D_2O) \rightarrow \quad (5c)$$

$$\nu_{OH}(HDO) \rightarrow \delta_{HDO}(\upsilon=2) \rightarrow \nu_{OD}(HDO) \rightarrow \nu_{OD}(D_2O) \quad (5d)$$

If processes 5b and 5d are significant, the ν_{OD}(HDO) must be a short-lived intermediate because we see no ν_{OD}(HDO) in Figure 9.

In HDO/D_2O measurements (Figure 9), the instantaneous number of δ_{D_2O} excitations is at least 6 times greater than the number of ν_{OD} excitations. That means δ_{D_2O} cannot be generated solely by $\nu_{OD}(D_2O) \rightarrow \delta(D_2O)$. We need to consider more efficient way of generating δ_{D_2O} from ν_{OH}, for example, the intermolecular bend-to-bend transfer,

$$\nu_{OH}(HDO) \rightarrow \delta_{HDO}(\upsilon=2) \rightarrow \delta_{D_2O}(\upsilon=2) \rightarrow \quad (6a)$$

$$\nu_{OH}(HDO) \rightarrow \nu_{OD}(HDO) \rightarrow \delta_{HDO} \rightarrow \delta_{D_2O} \rightarrow \quad (6b)$$

Our observation of significant stretch-to-bend transfer contrasts sharply with the proposal[26] by Nienhuys et al., who state ν_{OH} decay in HDO/D_2O occurs by excitation of hydrogen bonds, at a level that may be sufficient to cause vibrational predissociation. The hydrogen bond mechanism was proposed primarily on the basis of two observations:[26] (1) the time delay between $\upsilon = 1$ disappearance and $\upsilon = 0$ appearance implied the existence of a daughter excitation with a lifetime in the 0.5−2.0 ps range. However, this daughter was not observed directly. (2) VER has an unusual temperature dependence, becoming slower as the temperature is increased. The slowing with increased temperature is associated with the weakening of hydrogen bonds with increasing temperature.

Neither observation is inconsistent with the stretch-to-bend transfer directly observed here. The first observation is completely consistent with our results, because we find the bend lifetime to be in the 0.6−1.2 ps range. The unusual temperature dependence would also be expected for stretch-to-bend coupling. The magnitudes of the anharmonic matrix elements which couple stretch, bend, and bath[5] would decrease with decreasing hydrogen bond strength in a similar way as matrix elements which couple stretch and hydrogen bonds. Notice that our results do not rule out the possibility that up to 20% of the ν_{OH} decay could occur by exciting hydrogen bonds.

E. Decay of ν_{OD} Excitations. The ~2 ps lifetime for ν_{OD}-(D_2O) is about twice the lifetime for ν_{OH}. Energy level diagrams for ν_{OD} decay of HDO and D_2O are shown in Figures 3b,d. In heavy water as in water, the bend first overtone lies within the stretch transition. In fact everything is much the same in heavy water as in water, except that all the vibrational frequencies are smaller by about $\sqrt{2}$. Owing to the $(\omega)^{-1/2}$ frequency dependence of the creation and annihilation operators[55] in the anharmonic matrix elements which couple water stretch and bend excitations, this situation would simply lead to a VER lifetime for $\nu_{OD}(D_2O)$ which is a factor of 2 longer than for H_2O, as was seen here. We do not have any data for ν_{OD}(HDO), which Rey and Hynes predicted to have a 24 ps lifetime.[22] However our experiments would suggest that ν_{OD}(HDO) produced in a sea of D_2O would not be long-lived. It would decay rapidly by intermolecular transfer to the surrounding D_2O.

6. Summary and Conclusion

These are the first detailed measurements of VER in water and heavy water, and the first direct detection of daughter vibrational excitations generated by stretch decay in water and HDO/D_2O. Our direct observation of substantial bend generation in HDO/D_2O rules out the possibility that the hydrogen bond excitation process proposed by Nienhuys et al.[26] is dominant, and reveals some problems in the potential surface used for water VER calculations,[22] which underestimated the rates of energy transfer from the HDO solute to the D_2O solvent, in both stretch-to-stretch and bend-to-bend transfer processes.

Three processes cause time dependence evolution of the shape of the stretch transition in water. These are frequency-dependent VER, the dynamic Stokes shift, and spectral diffusion. As a result of the dynamic Stokes shift, the vibrational energy migration that causes the fast downhill spectral diffusion slows down after ~0.5 ps, so that frequency-dependent VER rates can affect the shape of the spectrum of ν_{OH} excitations. The longer lifetime of excitations on the blue edge of the stretching band causes an overall shift toward the blue at longer times. Woutersen et al.'s pump−probe experiments[25] on HDO/D_2O were the first to see the dynamic Stokes shift, but it is tricky to extract this effect from pump−probe experiments, as illustrated by the fact that Gale et al.'s experiments[12] missed it. The IR−Raman experiment makes seeing the Stokes shift much easier. Spectral diffusion in water in the uphill direction (from red to blue) is about the same as reported[12] for HDO/D_2O, but spectral diffusion in water in the downhill direction is far faster. Since fast vibrational hopping occurs in water but not in dilute solutions of HDO/D_2O, the fast downhill process is attributed to vibrational hopping to sites with different local structures and the slower downhill process is attributed to dynamic structural evolution.

The IR−Raman technique provides a great deal of new information about these very interesting fundamental processes in water, heavy water, and HDO/D_2O. Clearly much more remains to be done, including more detailed studies of the dependence on pump wavelength, isotopic composition and temperature, and the possibility of anti-Stokes detection of water librational excitations produced by VER.

Acknowledgment. This material is based on work supported by the National Science Foundation under award number DMR-9714843, and by the Air Force Office of Scientific Research under contract F49620-97-1-0056. L.K.I. acknowledges support from an AASERT fellowship, DAAG55-98-1-0191, from the Army Research Office. We thank the referee for insightful suggestions.

References and Notes

(1) Seilmeier, A.; Kaiser, W. Ultrashort Intramolecular and Intermolecular Vibrational Energy transfer of Polyatomic Molecules in Liquids. In *Ultrashort Laser Pulses and Applications*; Kaiser, W., Ed.; Springer-Verlag: Berlin, 1988; Vol. 60, p 279.
(2) Laubereau, A.; Kaiser, W. *Rev. Mod. Phys.* **1978**, *50*, 607.
(3) Hofmann, M.; Graener, H. *Chem. Phys.* **1995**, *206*, 129.
(4) Hofmann, M.; Zürl, R.; Graener, H. *J. Chem. Phys.* **1996**, *105*, 6141.
(5) Kenkre, V. M.; Tokmakoff, A.; Fayer, M. D. *J. Chem. Phys.* **1994**, *101*, 10618.
(6) Oxtoby, D. W. Vibrational Population Relaxation in Liquids. In *Photoselective Chemistry Part 2*; Jortner, J., Levine, R. D., Rice, S. A., Eds.; Wiley: New York, 1981; Vol. 47, p 487.
(7) Grote, R. F.; Hynes, J. T. *J. Chem. Phys.* **1980**, *73*, 2715.
(8) Grote, R. F.; Hynes, J. T. *J. Chem. Phys.* **1981**, *74*, 4465.
(9) Voth, G. A.; Hochstrasser, R. M. *J. Phys. Chem.* **1996**, *100*, 13034.
(10) Laenen, R.; Rauscher, C.; Laubereau, A. *J. Phys. Chem. B* **1998**, *102*, 9304.
(11) Laenen, R.; Rauscher, C.; Laubereau, A. *Phys. Rev. Lett.* **1998**, *80*, 2622.
(12) Gale, G. M.; Gallot, G.; Hache, F.; Lascoux, N.; Bratos, S.; Leicknam, J.-C. *Phys. Rev. Lett.* **1999**, *82*, 1068.
(13) Woutersen, S. Femtosecond vibrational dynamics hydrogen-bonded systems. Ph.D. Thesis, FOM-Institute for Atomic and Molecular Physics, Amsterdam, 1999.
(14) Maroncelli, M.; Fleming, G. R. *J. Chem. Phys.* **1988**, *89*, 5044.
(15) Stratt, R. M.; Maroncelli, M. *J. Phys. Chem.* **1996**, *100*, 12981.
(16) Woutersen, S.; Bakker, H. J. *Nature* **1999**, *402*, 507.
(17) Nitzan, A. *Nature* **1999**, *402*, 472.
(18) Vodopyanov, K. L. *J. Chem. Phys.* **1991**, *94*, 5389.
(19) Herzberg, G. *Molecular Spectra and Molecular Structure II. Infrared and Raman Spectra of Polyatomic Molecules*; Van Nostrand Reinhold: New York, 1945.
(20) Rice, S. A. Conjectures on the Structure of Amorphous Solid and Liquid Water. In *Topics in Current Chemistry*; Schuster, P. e. a., Ed.; Springer: New York, 1975; Vol. 60, p 109.
(21) Graener, H.; Seifert, G.; Laubereau, A. *Phys. Rev. Lett.* **1991**, *66*, 2092.
(22) Rey, R.; Hynes, J. T. *J. Chem. Phys.* **1996**, *104*, 2356.
(23) Woutersen, S.; Emmerichs, U.; Bakker, H. J. *Science* **1997**, *278*, 658.
(24) Woutersen, S.; Emmerichs, U.; Nienhuys, H.-K.; Bakker, H. J. *Phys. Rev. Lett.* **1998**, *81*, 1106.
(25) Woutersen, S.; Bakker, H. J. *Phys. Rev. Lett.* **1999**, *83*, 2077.
(26) Nienhuys, H.-K.; Woutersen, S.; van Santen, R. A.; Bakker, H. J. *J. Chem. Phys.* **1999**, *111*, 1494.
(27) Anex, D. S.; Ewing, G. E. *J. Phys. Chem.* **1986**, *90*, 1604.
(28) Disselkamp, R.; Ewing, G. E. *J. Phys. Chem.* **1989**, *93*, 6334.
(29) Ambroseo, J. R.; Hochstrasser, R. M. *J. Chem. Phys.* **1988**, *89*, 5956.
(30) Hong, X.; Chen, S.; Dlott, D. D. *J. Phys. Chem.* **1995**, *99*, 9102.
(31) Laenen, R.; Rauscher, C.; Laubereau, A. *Chem. Phys. Lett.* **1998**, *283*, 7.
(32) Bratos, S.; Leicknam, J.-C. *J. Chem. Phys.* **1994**, *101*, 4536.
(33) Deàk, J. C.; Iwaki, L. K.; Rhea, S. T.; Dlott, D. D. *J. Raman Spectrosc.* **2000**. In press.
(34) Iwaki, L.; Dlott, D. D. Vibrational Energy Transfer in Condensed Phases. In *Encyclopedia of Chemical Physics and Physical Chemistry*; Moore, J. H., Spencer, N. D., Eds.; Institute of Physics: Philadelphia, PA, 2000.
(35) Graener, H.; Laubereau, A. *Chem. Phys. Lett.* **1983**, *102*, 100.
(36) Weston, R. E. J. *Spectrochim Acta* **1962**, *18*, 1257.
(37) Bai, Y. S.; Fayer, M. D. *Phys. Rev. B.* **1989**, *39*, 11066.
(38) Silvestrelli, P. L.; Bernasconi, M.; Parrinello, M. *Chem. Phys. Lett.* **1997**, *277*, 478.

(39) Schrader, B. *Raman/Infrared Atlas of Organic Compounds*, 2nd ed.; VCH: Weinheim, 1989.
(40) Scherer, J. R.; Go, M. K.; Kint, S. *J. Phys. Chem.* **1974**, *78*, 1304.
(41) Deàk, J. C.; Iwaki, L. K.; Dlott, D. D. *Opt. Lett.* **1997**, *22*, 1796.
(42) Trebino, R.; DeLong, K. W.; Fittinghoff, D. N.; Sweetser, J. N.; Krumbügel, M. A.; Kane, D. J. *Rev. Sci. Instrum.* **1997**, *68*, 3277.
(43) Shapiro, S. L. *Ultrashort Light Pulses*; Springer-Verlag: Berlin, 1977; Vol. 18.
(44) Fendt, A.; Fischer, S. F.; Kaiser, W. *Chem. Phys.* **1981**, *57*, 55.
(45) Iwaki, L. K.; Dlott, D. D. *Chem. Phys. Lett.* **2000**. In press.
(46) Terhune, R. W.; Maker, P. D.; Savage, C. M. *Phys. Rev. Lett.* **1965**, *14*, 681.
(47) Kauranen, M.; Persoons, P. *J. Chem. Phys.* **1996**, *104*, 3445.
(48) Shen, Y. R. *Surf. Sci.* **1994**, *299/300*, 551.
(49) Deàk, J. C.; Iwaki, L. K.; Dlott, D. D. *J. Phys. Chem. A* **1998**, *102*, 8193.
(50) Gottfried, N. H.; Kaiser, W. *Chem. Phys. Lett.* **1983**, *101*, 331.
(51) Ziman, J. M. *Models of disorder*. *The Theoretical Physics of Homogeneously Disordered Systems*; Cambridge University Press: Cambridge, 1979.
(52) Grover, M.; Silbey, R. *J. Chem. Phys.* **1971**, *54*, 4843.
(53) Deàk, J. C.; Iwaki, L. K.; Dlott, D. D. *J. Phys. Chem.* **1998**, *102*, 8193.
(54) Velsko, S.; Hochstrasser, R. M. *J. Phys. Chem.* **1985**, *89*, 2240.
(55) Califano, S.; Schettino, V.; Neto, N. *Lattice Dynamics of Molecular Crystals*; Springer-Verlag: Berlin, 1981.